Greenstones as a source of hydrogen in cratonic sedimentary basins

Ian P. Hutchinson[1]*, Owain Jackson[2], Andrew E. Stocks[1], Andrew C. Barnicoat[1] and Stephen R. Lawrence[1]

[1]Natural Hydrogen Study Group (NHSG), Wallingford, Oxon, UK

[2]H2Au Ltd, Epsom, KT18 5AD, UK

IPH, 0000-0003-1380-1483; OJ, 0009-0005-0259-5460; AES, 0009-0003-2072-580X; ACB, 0009-0006-2744-0251; SRL, 0009-0001-3725-742X

*Correspondence: ian.hutchinson@nhsgconsultants.com

Abstract: A model is presented for the generation of natural hydrogen from cratonic basement rocks and its migration into the sediments of overlying cratonic basins. It is based on the 'discovery' of hydrogen at Bourakebougou in the Taoudeni Basin of Mali. In the 'Cratonic Greenstone Model', hydrogen is generated by the serpentinization of olivine-rich, ultramafic rocks contained within Precambrian 'greenstones'. The model requires a protolith (in greenstones), a supply of water (from groundwater), connecting faults to act as a plumbing system and an indurated sediment cover to retard hydrogen movement. Hydrogen is expelled into the overlying basin sediments, which form the host for hydrogen accumulations. The model describes a continental 'hydrogen system', which can form the basis for petroleum-type play-based hydrogen exploration in cratonic settings. Using play elements derived from the model, the Bourakebougou play fairway can be extended across the Taoudeni Basin >700 km northwards of the discovery.

In recent years, manufactured ('blue'/'green') hydrogen has become an accepted alternative energy fuel. However, there are still disadvantages in terms of its environmental impact and cost (US DoE 2020). Geological or natural hydrogen has been known about historically, for example, the gas burning at Mount Chimera in Turkey, thought to be the original source of the Olympic flame (Zgonnik 2020). Natural hydrogen is commonly referred to as 'gold' or 'white' hydrogen, and because it requires extraction rather than manufacture, it can be viewed as a primary energy source. If proven to occur in significant accumulations, natural hydrogen could become the 'green' successor to petroleum. In recent years, the prospect of natural hydrogen becoming an exploitable resource has become more feasible following the discovery at Bourakebougou in Mali (Prinzhofer *et al.* 2018; Maiga *et al.* 2023) and, more recently, drilling in Nebraska (Natural Hydrogen Energy LLC 2019). As a result, the quest for natural hydrogen has gathered momentum, with hydrogen exploration currently active in Africa, South America, Australia (Stalker *et al.* 2022), USA, France and Spain (Hand 2023).

Several sources of natural hydrogen are known or postulated but serpentinization is the only known subsurface reaction that demonstrably produces material volumes of natural hydrogen (Klein *et al.* 2020). Serpentinization requires water reacting with olivine or pyroxene in ultramafic rocks and this happens in several geological settings by interaction with seawater or meteoric water. These include oceanic spreading ridges (Worman *et al.* 2016) and oceanic transforms (Rüpke and Hasenclever 2017), passive margins (Albers *et al.* 2021), suprasubduction zones along active margins (Vitale Brovarone *et al.* 2020) and ophiolites where oceanic lithosphere has been obducted over continental lithosphere (Ulrich *et al.* 2020; Ellison *et al.* 2021). These are all 'oceanic' in the sense that the protolith for serpentinization is oceanic lithospheric mantle. In these usually inaccessible settings, exploration is still at a conceptual stage. However, exploration for hydrogen is already being carried out in continental settings in USA, Australia and Brazil, based on surface manifestations or reports of hydrogen in petroleum wells where the source of hydrogen is unknown or speculative. This makes it difficult to build genetic models to guide future exploration. In this paper, the 'oceanic' setting, where the hydrogen source is more predictable, is brought onshore to the craton in the middle of continents and a genetic model is derived for hydrogen exploration.

In the model, natural hydrogen is generated from cratonic basement rocks and migrates into the sediments of overlying cratonic basins. It is based on the discovery of hydrogen at Bourakebougou in southern Mali (Prinzhofer *et al.* 2018; Maiga *et al.* 2023) where hydrogen is being recovered from

From: Kilhams, B., Holford, S., Gardiner, D., Gozzard, S., Layfield, L., McLean, C., Thackrey, S. and Watson, D. (eds) 2024. *The Impacts of Igneous Systems on Sedimentary Basins and their Energy Resources*. Geological Society, London, Special Publications, **547**, 511–525.
First published online February 7, 2024, https://doi.org/10.1144/SP547-2023-39

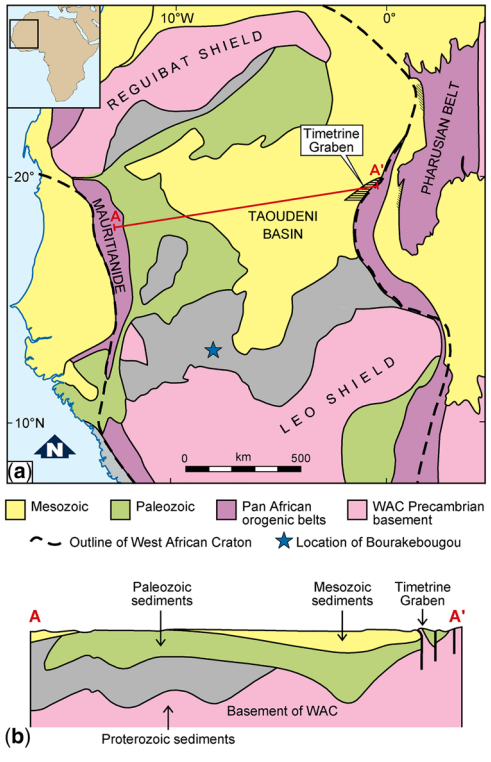

Fig. 1. The Taoudeni Basin. (**a**) Outcrop geology of the Taoudeni Basin and basement of the West African Craton with peripheral Pan-African orogenic belts. (**b**) Profile A–A' across the Taoudeni Basin showing Proterozoic to Mesozoic sediment fill. Source: modified after Guiraud *et al.* 2005.

Neoproterozoic carbonate and clastic sediments of the intracratonic Taoudeni Basin (Fig. 1). In the 'Cratonic Greenstone Model', hydrogen is generated by the serpentinization of olivine-rich ultramafic rocks contained within Precambrian 'greenstones' (for examples, see Vearncombe *et al.* 1986; de Wit and Ashwal 1995; Anhaeusser 2014). The model describes a continental 'hydrogen system', which forms the basis for petroleum-type play-based hydrogen exploration in cratonic settings. It should be noted that other sources of natural hydrogen are possible, such as radiolysis of water (Boreham *et al.* 2021) and mantle degassing (Zgonnik 2020).

Serpentinization

Serpentinization is a metamorphic reaction whereby water hydrates olivine and pyroxene contained within ultrabasic rocks (the 'protolith'). The reaction is not simple due to the impact of Mg–Fe solid solution in both reactant and product minerals (Evans 2008; Lazar 2020). The overall reaction can be simplified to

$$\begin{aligned} 6[(Mg1.5Fe0.5)SiO_4](\text{olivine}) + 7H_2O \\ = 3[Mg_3Si_2O_5(OH)_4](\text{serpentine}) \\ + Fe_3O_4(\text{magnetite}) + H_2. \end{aligned} \quad (1)$$

From the perspective of hydrogen generation, the key aspect of the reaction can be further simplified to the oxidation of ferrous to ferric iron by the reduction of water to hydrogen:

$$3FeO_{(\text{silicate})} + H_2O = Fe_3O_4 + H_2. \quad (2)$$

Conditions are driven to those of hydrogen stability by a series of reactions involving the control of silica activity, Mg–Fe distribution in mineral solid solutions and hydrogen activity (Lazar 2020). The main controls on serpentinization, and therefore the rates and volumes of hydrogen production, are petrological composition of the protolith, olivine composition (Fe v. Mg), effective grain size, temperature and water–rock ratio.

Although the serpentinization reaction can proceed over a wide range of temperatures, the optimal temperatures for significant hydrogen production rates and volumes lie between 200 and 300°C (e.g. Klein *et al.* 2013) (Fig. 2). This is the temperature bracket (or 'hydrogen generation window') invoked for the high-temperature serpentinization model presented here.

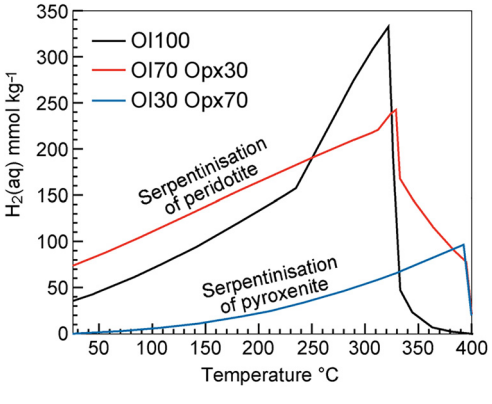

Fig. 2. The serpentinization reaction. Modelled concentrations of hydrogen at equilibrium between ultramafic mineral assemblages and an aqueous fluid at a pressure of 50 MPa (corresponding to a depth of *c.* 2 km) as a function of temperature. Water–rock ratio is unity. Ol100 = 100% olivine; Ol70 Opx30 = 70% olivine 30% pyroxene; Ol30 Opx70 = 30% olivine 70% pyroxene. Source: adapted from Klein *et al.* (2013).

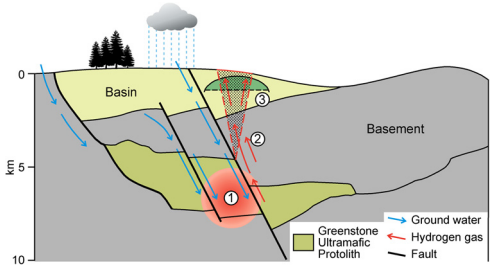

Fig. 3. The Cratonic Greenstone Model. (1) Hydrogen is generated from the protolith as a product of serpentinization. (2) Hydrogen migrates upwards along faults/fractures and through porous rocks/sediments. (3) Hydrogen becomes trapped in the sediments and forms accumulations. Source: the authors.

The Cratonic Greenstone Model: the geological set-up

The principle geological requirements for serpentinization and hydrogen production in the Cratonic Greenstone Model are highlighted in this section (Fig. 3).

Protolith

The protolith is formed by ultramafic rocks contained within cratonic greenstone belts of Precambrian basement. Greenstone belts are mega-scale components of the granite–greenstone terrains that make up Archean and Paleoproterozoic cratons (e.g. the Pilbara Craton of Australia; Fig. 4a). Thus, they occur in cratons on every continent and often form the basement to younger cratonic basins (Anhaeusser 2014). Greenstones are the 'ophiolites' of the 'early Earth' formed between granitic complexes in a pre-plate tectonic cratonization process (Vearncombe *et al.* 1986; de Wit and Ashwal 1995). The igneous rocks of greenstones can be broadly equated to the oceanic mantle–crust sequences of Phanerozoic ophiolites with mainly intrusive ultramafic components (e.g. the Paleoproterozoic Birimian greenstones of West Africa; Fig. 4b) (Dabo *et al.* 2017).

Greenstone belts are large-scale features (on the scale of hundreds of kilometres), usually longer than they are wide, giving the impression of being squeezed between the granitic complexes (see Fig. 4a). They tend to have an overall synformal form but are usually internally structurally complex (Vearncombe *et al.* 1986; de Wit and Ashwal 1995). Their internal structure is the product of a multi-phase deformational history involving low-angle thrusts and recumbent folds superimposed by isoclinal folds resulting in fold interference patterns (Baltazar and Lobato 2020; Bogossian *et al.* 2020). Often, a late-phase of strike–slip movement is recognized along pre-formed shear zones (Dirks *et al.* 2002).

The igneous rocks of greenstones include olivine-rich extrusives such as komatiites (mostly in the Archean) and intrusive bodies such as peridotites and dunites. These are usually metamorphosed between greenschist and granulite facies but, in the absence of water, olivine is stable to the highest

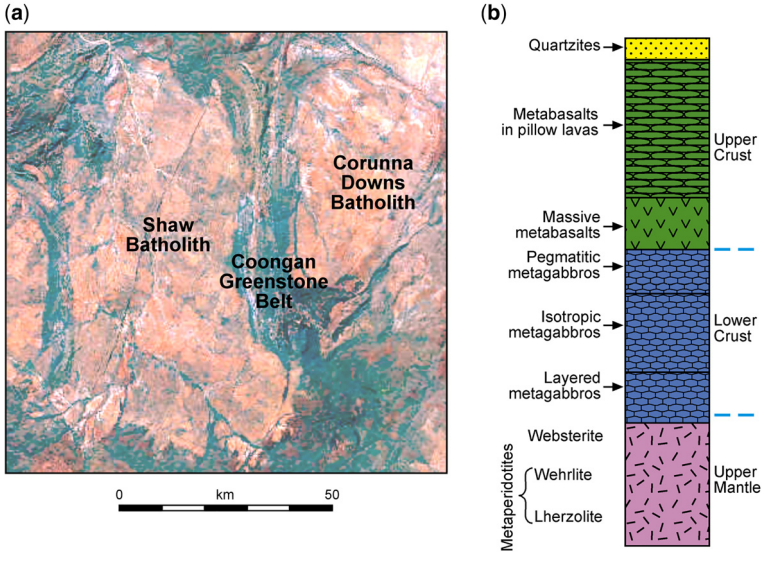

Fig. 4. Greenstones. (**a**) Satellite image of the Pilbara Craton showing greenstone belts (dark colours) situated between granite complexes (pink). (**b**) Birimian greenstone sequence based on Mako greenstone belt of the West African Craton. Source: adapted from Dabo *et al.* (2017).

metamorphic grades and magmatic conditions. The ultramafic rocks of greenstones will have undergone earlier phases of serpentinization (e.g. Blais and Auvray 1990; Rintamäki 2016), so that the greenstone protolith can be expected to be already partially serpentinized. However, in most cases they have retained sufficient remnant olivine content to enable later phases of serpentinization (Dabo *et al.* 2017, p. 133 for example).

Water supply

A 'body of water' is required to supply the water for the serpentinization reaction. In the cratonic setting, groundwater provides a ready supply of water charged by meteoric water from direct precipitation and/or by surface drainage. In cratonic basins, the groundwater can be derived from distant mountains and may take tens of thousands of years to charge aquifers in the basin (e.g. the water discharging in the oases of southern Tunisia fell as rain over 100 000 years BP in the southern Atlas more than 800 km away; GASPAL 2001). In the Sahara, extensive palaeo-groundwater reserves are found in large intracratonic sedimentary basins charged when the climate was wetter than the present day. In these basins, freshwater is known to occur in aquifers up to depths of 2000 m (GASPAL 2001). As detailed later, the water supply has to be sufficient to maintain continuous water–protolith contact.

Sedimentary basin cover

The occurrence of a sediment cover above the basement containing the protolith is a necessary requirement in this model for two reasons:

(1) The mobility of the hydrogen molecule (see later) means that preservation risks are reduced when the source has been active in geologically recent times and the basin sediments are of low-enough permeability to prevent or slow down the movement of hydrogen to the surface. The basin sediments will also form the host (or 'reservoir') for the hydrogen. Therefore, older (e.g. Proterozoic–Lower Paleozoic), more diagenetically altered basin sediments with low permeabilities are preferred for hydrogen retention.

(2) The basin sediments form a thermal blanket allowing the underlying basement protolith to achieve the required serpentinization temperatures by burial under 'normal' cratonic basal heat flow regimes (i.e. depths of 6–11 km for geothermal gradients of 25–30°C km^{-1}).

Sediment cover on cratons can be in the form of intracratonic basins (Allen and Armitage 2012), rift–sag basins (e.g. Jinhu *et al.* 2020) or lithospheric fold basins (Cloetingh and Burov 2011). They can also form along the edges of cratons in relation to younger orogenies (e.g. pro- and retro-foreland basins; Naylor and Sinclair 2008). For the reasons outlined above, the emphasis here is on older (Proterozoic–Lower Paleozoic) basins with a well-compacted or indurated sediment fill.

Cratonic faults

Faults are required to form the plumbing system connecting the water source (i.e. the groundwater zone) to the protolith deep within the basement. Cratons are by definition considered tectonically stable but major fault systems are often recognized crossing cratons, for example, the Perimbo fault of the Parana Basin (Rostirolla *et al.* 2003), the Tarim basin (Deng *et al.* 2019), the Tanlu fault of the North China Craton (Peng *et al.* 2022) and the Koolyanobbing shear zone of the Yilgarn Craton (Libby *et al.* 1991). Intracratonic faults are usually inherited from cratonization tectonics and re-activated by far-field deformation associated with younger (sometimes much younger) orogenic episodes. Often, these form major strike–slip systems subject to repeated episodes of transpressional and/or transtensional re-activation depending on the regional stress orientation (e.g. Deng *et al.* 2019).

For the model, the important property of faults is their permeability and capacity to allow water flow. The mechanical movement along faults introduces permeability heterogeneities and anisotropies, which can often have an impact on regional groundwater flow (Bense *et al.* 2013). Fault zones can have a permeability structure suggestive of complex conduit–barrier systems in which along-fault flow is promoted and across-fault flow is impeded (Barnicoat *et al.* 2009; Bense *et al.* 2013). In this way, fault zones can form hydraulic conduits connecting shallow to deep geological environments. Furthermore, it has been shown that dilatant shear failure along fault zones is more likely to result in permeability enhancement and focused fluid flow in low-porosity rocks like those of indurated basin sediments (Sheldon *et al.* 2006). Trickle flow of water through carrier beds and matrix porosity could contribute to low-level serpentinization. However, it is the huge quantity of water that these fault systems facilitate that allows the generation of economic volumes of hydrogen. It must also be recognized that these same fault systems present a risk of hydrogen loss.

The Cratonic Greenstone Model: the 'trigger' (activating the source)

As described, serpentinization requires an effective supply of water interacting with the olivine-rich

protolith at optimum temperatures of 200–300°C (although longer, slower generation at lower temperatures, with lower yields per kilogram of protolith is also possible). The key to generating significant volumes of hydrogen efficiently and in a timely manner in the subsurface is for meteoric water to access deep within the basin and the underlying basement down to the hydrogen generation window. Meteoric water charge of the groundwater zone can be along the basin margin ('topographically driven system') and/or via fault systems within the basin ('fault-driven system'). The fault-driven system is considered the most likely to reach the depths required and single- or multi-pass convective flow may play an important role. Groundwater forms a readily available body of water in cratonic settings, and basement faults, penetrating from deep to shallow levels (or to the surface), can form an effective plumbing system (Fig. 3).

To increase the chances of retaining hydrogen in the subsurface, the model requires that the link between the groundwater and the protolith is made in geologically recent times (possibly the last million years). In this case, it is preferable that the connecting faults have been neo-tectonically activated in order to create, or refresh, the permeable pathways, to focus water flow from the groundwater zone into deep basement aquifers, and thereby trigger a new phase of serpentinization.

The Cratonic Greenstone Model: the '3Rs' (reaction, release and retention)

Hydrogen generation

As noted earlier, serpentinization is chemically a complex process and textures within serpentinized peridotites indicate that it is also physically complex. The presence of fibrous serpentine in veins as well as mesh-textured replacement of primary minerals suggest that initial fluid access via fractures (e.g. Frost *et al.* 2013) is succeeded by more massive replacement. It is possible that the initial stages of reaction are accompanied by a volume increase facilitating fracturing and enhancing permeability. Fracturing may also occur after earlier, mesh-textured serpentinization (Rouméjon *et al.* 2015). However, significant volume increase associated with serpentinization (suggested by simple mass balance) is not evident and the changes in bulk chemistry needed for isovolumetric serpentinization are not observed (Evans *et al.* 2013).

Modelling of serpentinization leading to hydrogen generation assumes that the system is internally buffered; that is, reactions between the minerals in the rock control the fluid chemistry and hence the fluid–rock ratio is low (Sleep *et al.* 2004; Evans *et al.* 2013; Lazar 2020). Under such circumstances, fluid pressures may be lithostatic, or if fluid flow along faults is pulsed, varying between lithostatic and hydrostatic. The hydrogen, when generated, is likely to be in aqueous solution given the depths envisaged for the protolith (*c.* 7–10 km to attain suitable temperatures) and the solubility of hydrogen (Bazarkina *et al.* 2020; Lazar 2020). Hydrogen solubility in water is illustrated in Figure 5a, and Figure 5b shows the hydrogen activity in equilibrium with serpentinizing rock, which controls aqueous silica activity and hence hydrogen activity via the aqueous silica–fayalite(iron olivine end member)–magnetite buffer. The conditions under which a gaseous hydrogen phase will occur in aqueous systems are depicted in Figure 5b. Lazar (2020) shows that a hydrogen gas-phase is to be expected at temperatures

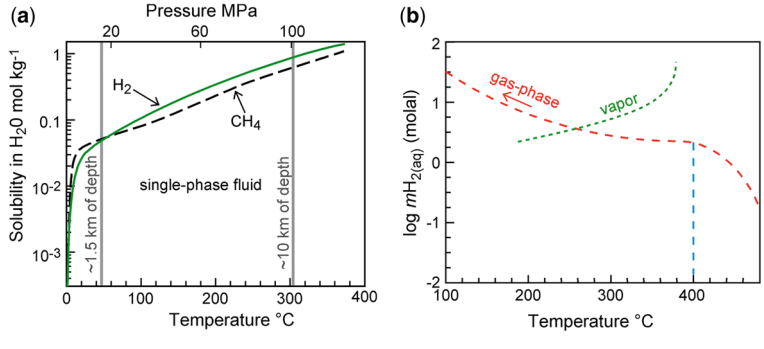

Fig. 5. Hydrogen generation and expulsion. (**a**) Solubility of H_2 and CH_4 in water along a hydrostatic pressure gradient. At conditions above the solubility curves (at the top left of the plot) a gas-phase is present in equilibrium with a water phase. Note the logarithmic solubility scale. (**b**) Modelled hydrogen activity in equilibrium with serpentinised peridotite at 200 MPa (*c.* 8 km depth) as a function of temperature. Changes in slope represent changes in mineral assemblage. The green line marks the limit of hydrogen solubility in aqueous fluid – to the left of the plot, a hydrogen-rich gas-phase is present (i.e. below *c.* 250°C). Source: (a) modified from Bazarkina *et al.* (2020); (b) modified from Lazar (2020).

below 250°C. Therefore, depending on the temperature (and depth) of serpentinization, hydrogen may be generated *in situ* as a gas-phase ($T < 250$°C) or in solution in an aqueous phase, separating from it when the temperature drops below 250°C.

Given the likely permeability of the basement containing the protolith, water ingress is expected to take place along (down) faults, particularly if they are active, and likewise the fluid and its contained or accompanying hydrogen is likely to migrate at least initially up the faults. Fluid flow in static basement faults (typically more permeable than the surrounding basement) will be convective with both up- and down-flows along its length (e.g. Zhao *et al.* 2003).

Hydrogen migration and entrapment

As a free gas, diatomic hydrogen will migrate and accumulate through the porous medium of rocks and sediments in the same way as hydrocarbon gases. However, the smaller molecular mass of hydrogen renders it more mobile than other gases. Hydrogen is soluble and the gas molecules can also migrate by diffusion. The hydrogen molecule is one of the most diffusive molecules. In this section, the movement and sealing potential of hydrogen in the subsurface is compared with that of natural gas (methane) and helium, a gas sometimes associated with hydrogen.

The mechanisms by which gas molecules can be transported through porous media are:

- advection in the gas-phase driven by pressure (buoyancy) and described by Darcy's Law;
- advection in solution also driven by pressure gradients; and
- diffusion in solution at the molecular level, driven by concentration gradients and described by Fick's Law.

All three mechanisms can operate when hydrogen moves through the subsurface (Fig. 6). Gas advecting in solution, or through diffusion, will exsolve and become gas-phase as maximum solubility levels are breached at lower temperatures and pressures (depths).

Bazarkina *et al.* (2020) show that raising temperatures from 150 to 300°C or increasing pressure from 30 to 200 MPa increases the solubility of hydrogen in water by a factor of about 2. The water content of hydrogen-rich vapour in equilibrium with the liquid water changes much more than the composition of the coexisting liquid, especially at low pressures. Thus, differing geothermal gradients will not have a major impact on the temperature at which a gas-phase forms in water–hydrogen systems. The salinity of the water also impacts hydrogen solubility and would increase the depth (and temperature) at which a gas-phase formed (Lopez-Lazaro *et al.* 2019). Note that Lopez-Lazaro *et al.* (2019) show solubility increasing significantly with depth. This is at very shallow, cool conditions. We envisage serpentinization, causing hydrogen generation, under rock-dominated, lithostatically pressured conditions and the transition to hydrostatically pressured conditions facilitates gas-phase formation.

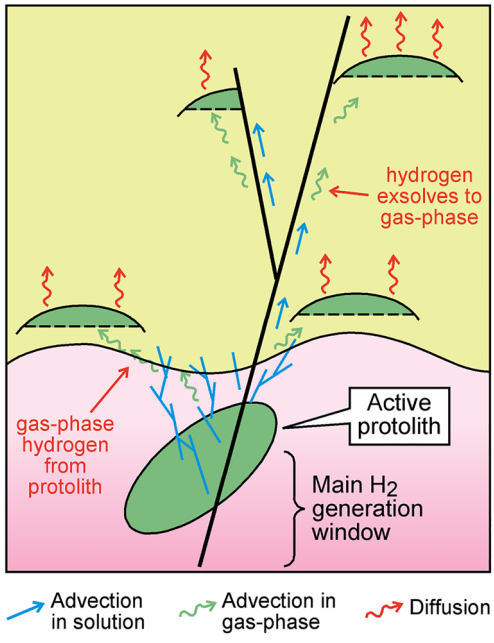

Fig. 6. Schematic diagram showing hydrogen migration in the subsurface by advection in gas-phase, advection in solution and diffusion. Source: the authors.

Advection in the gas-phase will be the most efficient migration process and Darcy-type flow will dominate up to the point where the capillary forces in the pores in low-permeability rocks become too strong to be overcome by the buoyancy pressure. This is demonstrated in Figure 7, which plots estimated attainable gas column heights (up to a capillary pressure threshold) against pore-throat size (based on a notional gas-water contact at 1000 m). An indication of typical pore-throat sizes for a range of lithologies is shown. This illustrates that, as a consequence of its greater buoyancy, marginally smaller column heights are required by hydrogen than methane to overcome capillary pressures for given pore-throat sizes, and demonstrates that substantial hydrogen gas accumulations can be retained by capillary forces.

Advective flow will be re-established if the buoyancy pressure overcomes the mechanical sealing strength of the rock. A comparison of relative column heights of hydrogen, helium and methane

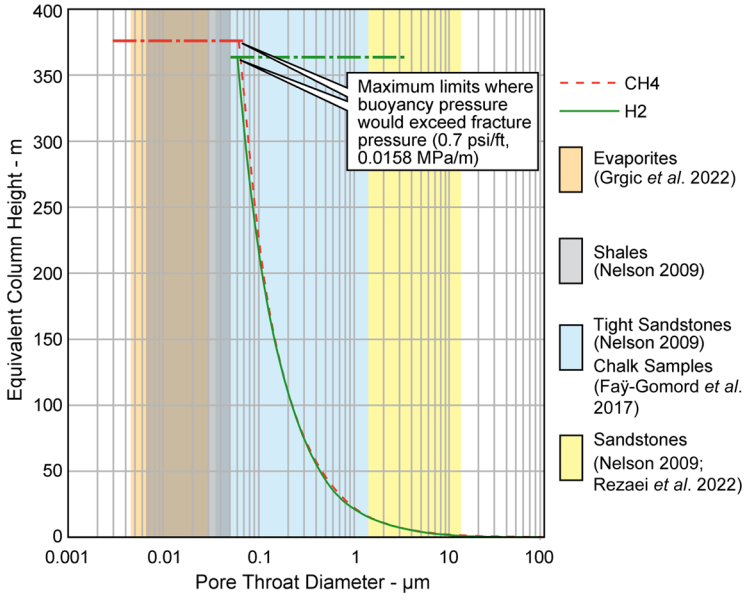

Fig. 7. Attainable gas column heights (based on capillary thresholds and buoyancy effects with a gas-water contact at 1000 m) plotted against pore-throat diameters for evaporite and clastic lithologies. Source: the authors.

against a nominal fracture gradient of 0.7 psi ft^{-1} is shown in Figure 8. This highlights that maximum columns for hydrogen and helium are only marginally less than those of methane (for a given contact depth).

A standard approach for discriminating between single-phase gas flow regimes in porous media uses the Knudsen number. This relates flow characteristics to the mean free path of the gas and the pore-throat size (known as 'characteristic size'; Roy *et al.* 2003; Sakhaee-Pour and Alessa 2022). The mean free path is a function of the density and viscosity, and will change with depth as temperature and pressure increase. In this way, the change in flow character with depth can be traced according to the concomitant change in mean free path. Darcy-type, advective flow breaks down when the Knudsen number passes the threshold between 'slip flow' and 'transition flow' at a value of 0.1. In Figure 9, this approach is used to estimate where, in pore-throat size v. depth terms, diffusion will become the more dominant flow regime for hydrogen, helium and methane. It can be seen that hydrogen will potentially be more restricted than methane in its advective flow at deeper levels.

Under subsurface multi-phase conditions there will be an additional restriction to advective flow imparted by the water occupying and restricting the pore space. In this case, the diffusion–advection boundary is displaced to larger pore-throat sizes. An estimated minimum likely displacement of this boundary for hydrogen is indicated in Figure 9. It should be emphasized that the Knudsen-based flow regimes are indicators of the likely mode of flow and not necessarily the rate of flow.

Ranges of pore-throat sizes for typical reservoir and sealing lithologies are plotted in Figure 9 including the 'reservoir' and 'caprock' of Sakhaee-Pour and Alessa (2022). For typical reservoir formations or aquitards (e.g. sandstones), it is expected that hydrogen will be more mobile than methane (e.g. up to two times reported by Lodhia and Clark 2022). However, the lithologies that form effective sealing formations (or aquicludes) for advective flow (shales and evaporites) are similar for hydrogen and methane. The other observation is that advective flow of both gases can become less effective at very shallow levels ($<$100 m), especially in more indurated sediments, due to the rapid increase in mean free paths.

When advection ceases due to pore-throat size restriction (i.e. the gas can be considered sealed), diffusion will become the dominant flow mechanism. Diffusion coefficients for gases in pure water indicate hydrogen to be approximately 2.8$\times$ more diffusive than methane at 25°C but 0.7$\times$ that of helium. However, the effective diffusion coefficients are significantly restricted by the tortuosity of the connected pore water network. Further, the rate of diffusion, the diffusion flux, is constrained by distance and the concentration gradient of the gas in solution across that distance. Attempts made to quantify diffusive losses from hydrocarbon gas

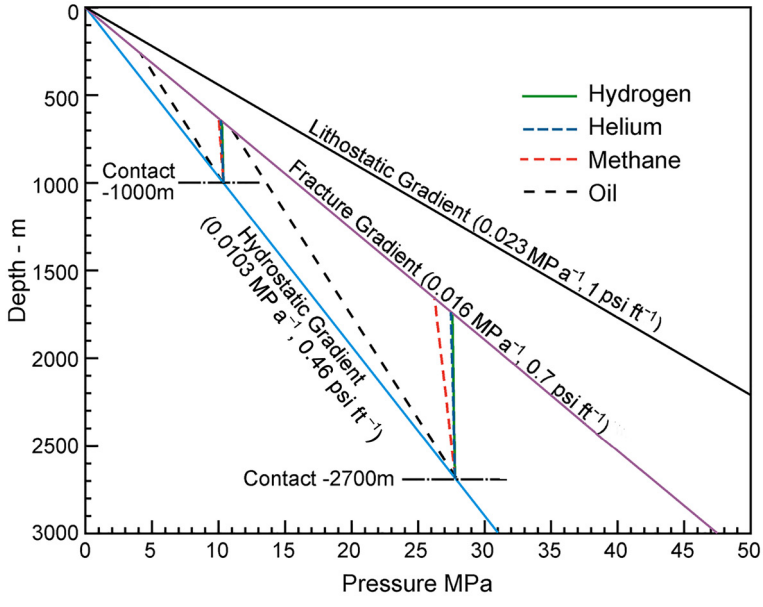

	Contact depth - m	
	1000	2700
Press. Grad. - MP a^{-1}		
H_2	0.00007	0.00017
He	0.00015	0.00034
CH4	0.00059	0.00137
Oil	0.00837	0.00837

Fig. 8. Limiting effects of fracture pressure on maximum attainable column heights for hydrogen, helium, methane and oil. Source: the authors.

accumulations indicate that losses could be significant over geological timescales given certain conditions (e.g. Montel *et al.* 1993; Nelson and Simmons 1995). However, the existence of substantial hydrocarbon gas accumulations is well known, and diffusive losses have not been considered a significant concern. Information on diffusive losses of hydrogen over historical timescales is becoming available from hydrogen storage studies (see Hemme and Van Berk 2018; Perera 2023).

However, a key factor in the magnitude of diffusive losses is the relatively low solubility of both hydrogen and helium compared with methane. Whilst hydrogen and helium have comparable levels of solubility, methane is indicated to be some 14 times more soluble than hydrogen at surface conditions (Kaye and Laby 1986, p. 219). It has been concluded that little risk of significant diffusive losses is indicated (Monge and Vayssaire 2022) and this would be particularly so where thick and/or well-indurated sealing formations are present.

The 'cratonic' hydrogen system and exploration play

The Cratonic Greenstone Model describes a 'hydrogen system' analogous to the 'petroleum system' used in understanding petroleum generation and migration (Magoon and Dow 1994). In the case of the 'cratonic' hydrogen system, the 'source rock' is formed by the greenstone (ultramafic) protolith (with a water supply from groundwater) and the 'reservoir' (or aquitard) by a host lithology within the indurated sedimentary column of the overlying cratonic basin. Also, in some cases, the reservoir could be in fractured basement rocks between the protolith and the basin sediments.

The petroleum system provides information on the source–migration part of the 'source–migration–trap' paradigm, which has been used successfully over decades to guide petroleum exploration. The other useful concept is that of the 'exploration play', which recognizes the combination of geological

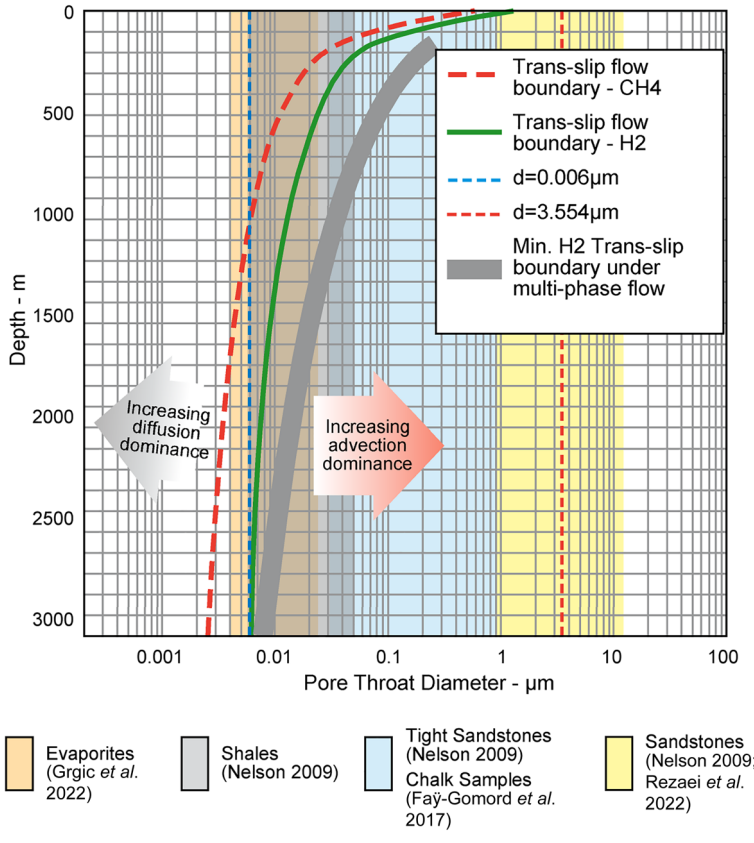

Fig. 9. Indication of single-phase flow regimes in the subsurface for hydrogen and methane as function of depth and pore-throat diameter. Shows estimated advection/diffusion transition for hydrogen shifted for multi-phase flow. $d =$ 0.006 µm is the 'caprock' of Sakhaee-Pour and Alessa (2022); $d = 3.554$ µm is the 'reservoir' of Sakhaee-Pour and Alessa (2022). These are typical pore-throat diameters for evaporites and clastic lithologies. Source: the authors.

conditions controlling the accumulation of petroleum in a particular province or cluster of oil/gasfields (Allen and Allen 2005). Transferring this approach to natural hydrogen, the Cratonic Greenstone Model can be used to identify the first-order play elements to guide natural hydrogen exploration in cratonic settings. As highlighted, these are: protolith, water supply, plumbing system and indurated basin sediments. The migrational/sealing and therefore trapping processes are the same for hydrogen and methane. Trapping scenarios will be formed by the reservoir–seal (or aquitard–aquiclude) having a suitable structural or stratigraphic trapping configuration.

Hydrogen exploration in cratons

The Cratonic Greenstone Model can be used for natural hydrogen exploration in cratonic settings worldwide. In this section, the first-order play elements derived from the model have been applied to the southern West African Craton and Taoudeni Basin using a mapped based screening process.

Protolith

The greenstones of Archean and Proterozoic greenstone belts comprise extrusive and intrusive igneous rock sequences with associated sediments. These are exposed in cratonic basement terrains and can also form the basement to younger cratonic basins. Greenstone belts have a recognizable outcrop pattern in the map domain but the key to potential protolith discrimination within the greenstone belt lies in the analysis of the available geological information to identify olivine-rich rock units. Where they are located on the edge of cratonic basin cover, greenstones can be extrapolated along strike under sedimentary cover using geophysical data if available. With a high ultramafic rock content, their dominant signature will be a positive gravity response although this may be negated by the presence of associated less

dense sediments and serpentinized igneous rocks (Ranganai 2012). An additional diagnostic feature may be provided by the magnetic response of magnetite produced by serpentinization (Toft *et al.* 1990; Manuella and Carbone 2019).

The most likely source of the hydrogen at Bourakebougou is considered to be active serpentinization of a greenstone protolith within the 2.2–2.1 Ga Birimian greenstones of the Leo-Man Shield of the West African Craton (Fig. 10a; Dabo *et al.* 2017; Labou *et al.* 2020). Where exposed in the Mako region of eastern Senegal, the greenstones comprise meta-peridotites (including harzburgite, wehrlite and lherzolite), meta-gabbros and basalts (see Fig. 4b; Dabo *et al.* 2017; Labou *et al.* 2020). Wehrlites and dunites are reported in the greenstones of the Kadiolo and Boromo Belts to the south of the Taoudeni Basin in Burkino Faso (Labou *et al.* 2020).

The degree of serpentinization in Birimian greenstones is not widely reported but it has been recorded in Birimian greenstones at Mako (Labou *et al.* 2020), in the Kaya–Goren greenstone belt of Burkino Fasso (Zongo *et al.* 2016) and at Makalondi in Niger (Garba Saley *et al.* 2019). It is expected that this is early-phase serpentinization formed during initial oceanic spreading or in a supra-subduction zone setting.

Water supply

There is a well-developed groundwater system in southern Mali with aquifers in unconsolidated Cretaceous and Tertiary sediments, fractured Jurassic intrusive igneous rocks, inter-granular and fractured Neo-Proterozoic sediments and fractured basement (Traore *et al.* 2018). These aquifers have been charged during historical river flooding episodes

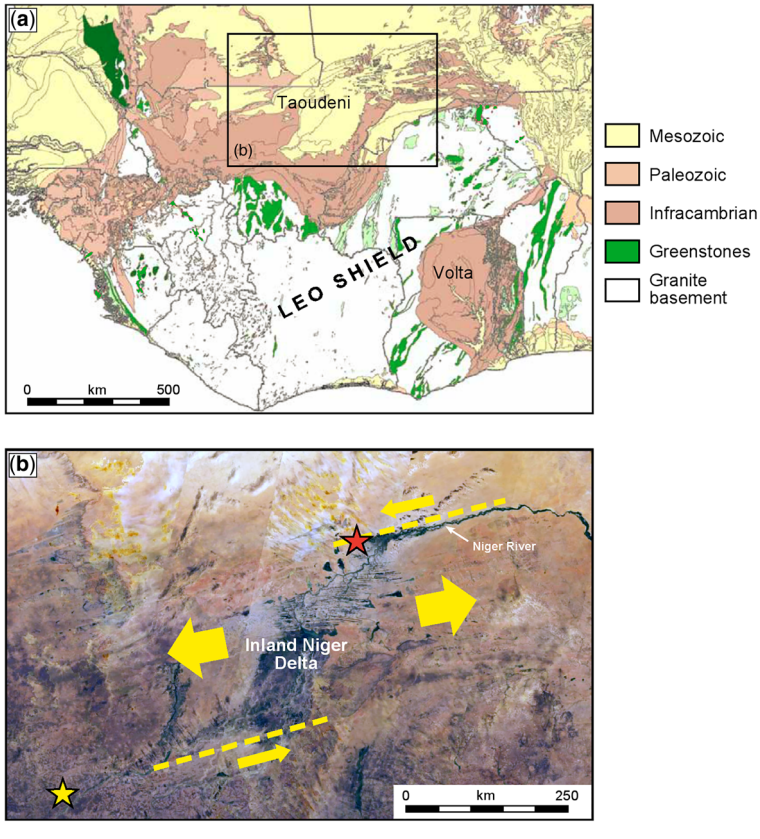

Fig. 10. Southern West African Craton and Taoudeni Basin. (**a**) Map-based presentation showing combined layers for greenstone protolith and intracratonic basin cover. (**b**) Sinistral pull-apart model for fault development in the southern Taoudeni Basin showing the fault architecture and water recharge area below the Inland Niger Delta. The hydrogen occurrences at Bourakebougou are shown with a yellow star and the burning 'fumaroles' of Lake Faguibine shown with a red star. Source: (a) the authors.

(of the Inland Niger River Delta), and directly from rainfall, during Holocene wet periods (GASPAL 2001).

Intracratonic sediment cover

Proterozoic and Paleozoic intracratonic basins are widely developed across Africa. Their hydrogen-retention capabilities have been enhanced by compaction and induration resulting from several phases of Paleozoic and Mesozoic burial and later episodes of metamorphism or metasomatism associated with igneous activity. These basins are ideal for capturing and focusing the hydrogen emanating from the underlying basement and avoiding direct loss into the atmosphere, as would be the case where the greenstones are in shallow or exposed basement.

The Taoudeni Basin covers a large part of the West African Craton with a Proterozoic to Tertiary sediment fill (see Fig. 1). In the southern Taoudeni Basin, Proterozoic, Infracambrian and Lower Paleozoic sediments form the main part of the cratonic cover section (Fig. 10a). Also, early Jurassic intrusives have played an important role in sediment diagenesis (Girard *et al.* 1989) and probably in forming seals or aquicludes to vertically moving hydrogen (Prinzhofer *et al.* 2018; Maiga *et al.* 2023). At Bourakebougou, reservoirs are formed by vuggy carbonates and sandstones (Prinzhofer *et al.* 2018). It should be noted that Prinzhofer *et al.* (2018)'s Reservoir-1 is within 100 m of the surface. The rapid increase of mean free path at shallow levels might explain the enhanced seal efficiency of near-surface formations, which may include laterites and/or ferricretes.

Neo-tectonic fault systems

Major intracratonic fault systems, controlled by the inherent cratonic structure, can be identified as lineaments and mapped faults on geological maps. Neotectonic activity along these fault systems can be analysed from seismic event records, topography and drainage patterns.

Major basement fault systems have been interpreted traversing the West African Craton and the Taoudeni Basin forming the ENE–WSW Guinea–Nubian Line of Lesquer and Moussine-Pouchkine (1980), Bellion *et al.* (1984), Guiraud *et al.* (1985) and Sauvage and Sauvage (1992), and the NE–SW Adrar–Guinea Line of Kahoui *et al.* (2008). Faults can be seen crossing the southern Taoudeni Basin (Fig. 10a), where they appear to have been re-activated several times in their geological history including Cretaceous extension to form the Nara (Bellion *et al.* 1984) and Timetrine graben and late Eocene inversion (Bellion and Guiraud 1988).

A phase of post-Villafranchian (i.e. early Pleistocene) faulting is recognized in the Nara–Lake-Faguibine–Daounas area (Sauvage and Sauvage 1992) and the indications are that this tectonic activity has continued into modern times. Recent movement on faults has affected the course of the Niger River (Blanck and Tricart 1990) and the formation of the Inland Niger Delta and Lake Faguebine (Guiraud *et al.* 1985; El Abbass *et al.* 1993). Modern seismic activity is known in the region including tremors in the vicinity of Timbuctoo in 1905 and 1984 (Sauvage and Sauvage 1992). A tectonic model is presented for Pleistocene to Recent strike–slip fault movement and sinistral pull-apart development in southern Mali (Fig. 10b), building on that proposed by Sauvage and Sauvage (1992). It is envisaged that the change in permeability induced by the recent fault activity would have allowed groundwater to access these faults, whilst acknowledging that they may contribute to an increased risk of hydrogen loss.

The Taoudeni Basin 'play'

Using the play elements as described, the Bourakebougou play fairway can be extended >700 km northwards of the Bourakebougou discovery within the Taoudeni Basin (see Fig. 10a). Neo-tectonic faults that form part of a strike–slip pull-apart system can be seen affecting a plumbing system over a large area for a groundwater system charged by surface drainage across the Inland Niger Delta (Fig. 10b). Greenstones can be extended northwards under basin cover on the basis of geophysical evidence of dense basement rock bodies (see Lesquer and Moussine-Pouchkine 1980; Sauvage and Sauvage 1992; El Abbass *et al.* 1993). Traps are formed by structures related to the cratonic faults and anticlinal structures formed by Pan-African foreland tectonics (Sauvage and Sauvage 1992).

Having extended the 'Bourakebougou play' northwards, physical signs of hydrogen have been investigated in order to de-risk the play. In the Daouna–Lake-Faguibine area, 'flammable gas' is reported emanating from fractures and so-called 'fumaroles' (Sauvage and Sauvage 1992) and the local population report luminous emissions at night (Sauvage and Sauvage 1992) (see Fig. 10b). In addition there is a more recent report of locals describing flammable gas seeping out of the ground (International Committee of the Red Cross Press Release 29 September 2021; https://www.icrcnewsroom.org/story/en/1968/mali-climate-change-transforms-lake-faguibine-into-desert-exiling-population). Another phenomenon observed in the area is that of underground fires whose origin has long been debated (Sauvage and Sauvage 1992; El Abbass *et al.* 1993; Svensen *et al.* 2003). It is proposed that these phenomena

can all be explained by the seepage of hydrogen from the ground. It is also notable that these seepages are in the vicinity of structures formed by Pan-African foreland tectonics and surface-expressed faults (Sauvage and Sauvage 1992).

Conclusions

A model is presented for the generation of natural hydrogen from cratonic basement rocks and its migration into the sediments of overlying cratonic basins. In the Cratonic Greenstone Model, hydrogen is generated by serpentinization of olivine-rich ultramafic rocks contained within greenstones of greenstone belts in Precambrian basement.

The model is based on the discovery of hydrogen at Bourakebougou in southern Mali where hydrogen is being recovered from Neoproterozoic carbonate and clastic sediments of the intracratonic Taoudeni Basin. The model requires a protolith (in greenstones), a supply of water (from groundwater), connecting faults to act as a plumbing system and an indurated sediment cover to retard hydrogen movement. Hydrogen is expelled from the source protolith into the overlying sediments which form the host for hydrogen accumulations. Unlike the petroleum system, hydrogen generation from serpentinization is expected to occur over much shorter timeframes and accumulations in the subsurface could be in a state of active replenishment from its source (Maiga *et al.* 2023).

The model describes a continental hydrogen system which can form the basis for play-based exploration across cratonic areas. First-order play elements have been identified and used to extrapolate the 'Bourakebougou play' across a large area of the Taoudeni Basin. The cratonic greenstone play is a new hydrogen exploration play which can be used to guide hydrogen exploration in any cratonic areas containing Archean or Paleoproterozoic greenstones with overlying basins.

Despite its success in petroleum exploration, the use of the play approach for natural hydrogen exploration has not been recorded in the public domain. This is partly due to the perceived differences in behaviour between hydrocarbon gases and hydrogen and how the respective systems work. To counter this, further research is required to advance the understanding of the hydrogen system focused on source (serpentinization, hydrogen generation and expulsion) and migration/sealing potential (hydrogen mobility under multi-phase advective flow and diffusion).

Acknowledgements Geoff Ellis (USGS) and an anonymous reviewer are thanked for their useful and constructive comments.

Competing interests The authors declare that they have no known competing financial interests or personal relationships that could have appeared to influence the work reported in this paper.

Author contributions **IPH**: conceptualization (equal), investigation (equal), writing – review & editing (equal); **OJ**: conceptualization (equal), investigation (equal), writing – review & editing (equal); **AES**: conceptualization (equal), investigation (equal), writing – review & editing (equal); **ACB**: conceptualization (equal), investigation (equal), writing – review & editing (equal); **SRL**: conceptualization (equal), investigation (equal), supervision (lead), writing – original draft (lead), writing – review & editing (equal).

Funding This research received no specific grant from any funding agency in the public, commercial, or not-for-profit sectors.

Data availability Data sharing is not applicable to this article as no datasets were generated or analysed during the current study.

References

Albers, E., Bach, W., Perez-Gussinye, M., McCammon, C. and Frederichs, T. 2021. Serpentinisation driven H_2 production from continental break-up to mid-oceanic ridge spreading: unexpected high rates at the West Iberia Margin. *Frontiers in Earth Science*, **9**, 1–24, https://doi.org/10.3389/feart.2021.673063

Allen, P.A. and Allen, J.R. 2005. *The Petroleum Play Basin Analysis: Principles and Applications*. Blackwell, Oxford.

Allen, P. and Armitage, J.J. 2012. Cratonic basins. *In*: Busby, C. and Azor, A. (eds) *Tectonics of Sedimentary Basins: Recent Advances*. Blackwell, Oxford, 602–620, https://doi.org/10.1002/9781444347166.ch30

Anhaeusser, C.R. 2014. Archaean greenstone belts and associated granitic rocks – a review. *Journal of African Earth Sciences*, **100**, 684–732, https://doi.org/10.1016/j.jafrearsci.2014.07.019

Baltazar, O.F. and Lobato, L.M. 2020. Structural evolution of the Rio das Velhas Greenstone Belt, Quadrilátero Ferrífero, Brazil: influence of proterozoic orogenies on its Western Archean gold deposits. *Minerals*, **10**, 983, https://doi.org/10.3390/min10110983

Barnicoat, A.C., Sheldon, H.A. and Ord, A. 2009. Faulting and fluid flow in porous rocks and sediments: implications for mineralisation and other processes. *Mineralium Deposita*, **44**, 705–718, https://doi.org/10.1007/s00126-009-0236-4

Bazarkina, E.F., Chou, I.-M., Goncharov, A.F. and Akinfiev, N.N. 2020. The behavior of H_2 in aqueous fluids under high temperature and pressure. *Elements*, **16**, 33–38, https://doi.org/10.2138/gselements.16.1.33

Bellion, Y. and Guiraud, R. 1988. Eocene compressive deformations West of Adrar des Iforas (Mali). *Comptes*

Rendus de l'Académie des sciences, Série II, **307**, 529–532.

Bellion, Y., Benkhelil, J. and Guiraud, R. 1984. Evidence for compressive deformations in the *Continental intercalaire* of the southern part of the Taoudenni basin (Eastern Hodh, Mauritania-Mali borders). *Bulletin de la Société géologique de France, Series 7*, **26**, 1137–1147, https://doi.org/10.2113/gssgfbull.S7-XXVI.6.1137

Bense, V.F., Gleeson, T., Loveless, S.E., Bour, O. and Scibek, J. 2013. Fault zone hydrogeology. *Earth-Science Reviews*, **127**, 171–192, https://doi.org/10.1016/j.earscirev.2013.09.008

Blais, S. and Auvray, B. 1990. Serpentinization in the Archean komatiitic rocks of the Kuhmo greenstone belt, eastern Finland. *The Canadian Mineralogist*, **28**, 55–66.

Blanck, J.-P. and Tricart, J.L.F. 1990. Some effects of neotectonics on the landforms in the region of the Central Delta of River Niger (Mali). *Comptes Rendus de l'Académie des sciences, Série II*, **310**, 309–313.

Bogossian, J., Hagemann, S.G., Rodrigues, V.G., Lobato, L.M. and Roberts, M. 2020. Hydrothermal alteration and mineralization in the Faina greenstone belt: evidence from the Cascavel and Sertão orogenic gold deposits. *Ore Geology Reviews*, **119**, 1–29, https://doi.org/10.1016/j.oregeorev.2019.103293

Boreham, C.J., Edwards, D.S. *et al*. 2021. Hydrogen in Australian natural gas: occurrences, sources and resources. *The APPEA Journal*, **61**, 163–191, https://doi.org/10.1071/AJ20044

Cloetingh, S. and Burov, E. 2011. Lithospheric folding and sedimentary basin evolution: a review and analysis of formation mechanisms. *Basin Research*, **23**, 257–290, https://doi.org/10.1111/j.1365-2117.2010.00490.x

Dabo, M., Aïfa, T., Gning, I., Faye, M., Ba, M.F. and Ngom, P.M. 2017. Lithological architecture and petrography of the Mako Birimian greenstone belt, Kédougou-Kéniéba Inlier, eastern Senegal. *Journal of African Earth Sciences*, **131**, 128–144, https://doi.org/10.1016/j.jafrearsci.2017.04.005

Deng, S., Li, H., Zhang, Z., Zhang, J. and Yang, X. 2019. Structural characterization of intracratonic strike-slip faults in the central Tarim Basin. *AAPG Bulletin*, **103**, 109–137, https://doi.org/10.1306/06071817354

de Wit, M.J. and Ashwal, L.D. 1995. Greenstone belts: what are they? *South African Journal of Geology*, **98**, 505–520.

Dirks, P.H.G.M., Jelsma, H.A. and Hofmann, A. 2002. Thrust-related accretion of an Archaean greenstone belt in the Midlands of Zimbabwe. *Journal of Structural Geology*, **24**, 1707–1727, https://doi.org/10.1016/S0191-8141(02)00002-0

El Abbass, T., Person, A., Gerard, M., Albouy, Y., Sauvage, M., Sauvage, J.-F. and Bertil, D. 1993. Geophysical and geological arguments for recent volcanic events in Faguibine Lake zone (Mali). *Comptes Rendus de l'Académie des sciences, Série II*, **316**, 1301–1310.

Ellison, E.T., Templeton, A.S., Zeigler, S.D., Mayhew, L.E., Kelemen, P.B. and Matter, J.M. and The Oman Drilling Project Science Party. 2021. Low-temperature hydrogen formation during aqueous alteration of serpentinized peridotite in the Samail ophiolite. *Journal of Geophysical Research: Solid Earth*, **126**, https://doi.org/10.1029/2021JB021981

Evans, B.W. 2008. Control of the products of serpentinization by the $Fe^{2+}Mg_{-1}$ exchange potential of olivine and orthopyroxene. *Journal of Petrology*, **49**, 1873–1887, https://doi.org/10.1093/petrology/egn050

Evans, B.W., Hattori, K. and Baronnet, A. 2013. Serpentinite: what, why, where? *Elements*, **9**, 99–106, https://doi.org/10.2113/gselements.9.2.99

Faÿ-Gomord, O., Soete, J. *et al*. 2017. Tight chalk: characterization of the 3D pore network by FIB-SEM, towards the understanding of fluid transport. *Journal of Petroleum Science and Engineering*, **156**, 67–74, https://doi.org/10.1016/j.petrol.2017.05.005

Frost, B.R., Evans, K.A., Swapp, S.M., Beard, J.S. and Mothersole, F.E. 2013. The process of serpentinization in dunite from New Caledonia. *Lithos*, **178**, 24–39, https://doi.org/10.1016/j.lithos.2013.02.002

Garba Saley, H., Konaté, M. and Soumaila, A. 2019. Nickel mineralizations of the Birimian greenstone belt of Makalondi (Liptako Province of Niger, West Africa). Presented at the 4th Colloquium of the International Geoscience Programme (IGCP638) in Algeria, University of Algiers USTHB, Algeria.

GASPAL (Groundwater as Palaeoindicator). 2001. *Groundwater: A Renewal Resource? Focus on Sahara and Sahel*. EC ENRICH/British Geological Survey, 1–17.

Girard, J.-P., Deynoux, M. and Nahon, D. 1989. Diagenesis of the upper Proterozoic siliciclastic sediments of the Taoudeni Basin (West Africa) and relation to diabase emplacement. *Journal of Sedimentary Research*, **59**, 233–248, https://doi.org/10.1306/212f8f58-2b24-11d7-8648000102c1865d

Grgic, D., Al Sahyouni, F., Golfier, F., Moumni, M. and Schoumacker, L. 2022. Evolution of gas permeability of rock salt under different loading conditions and implications on the underground hydrogen storage in salt caverns. *Rock Mechanics and Rock Engineering*, **55**, 691–714, https://doi.org/10.1007/s00603-021-02681-y

Guiraud, R., Issawi, B. and Bellion, Y. 1985. The Guineo-Nubian lineaments: a major structural zone of the African Plate. *Comptes Rendus de l'Académie des sciences, Série II*, **300**, 17–20.

Guiraud, R., Bosworth, W., Thierry, J. and Delplanque, A. 2005. Phanerozoic geological evolution of Northern and Central Africa: an overview. *Journal of African Earth Sciences*, **43**, 83–143, https://doi.org/10.1016/j.jafrearsci.2005.07.017

Hand, E. 2023. Hidden hydrogen. *Science (New York, NY)*, **379**, 630–636, https://doi.org/10.1126/science.adh1477

Hemme, C. and Van Berk, W. 2018. Hydrogeochemical modeling to identify potential risks of underground hydrogen storage in depleted gas fields. *Applied Sciences*, **8**, https://doi.org/10.3390/app8112282

Jinhu, D., Zecheng, W. *et al*. 2020. Discovery of intracratonic rift in the Upper Yangtze and its control effect on the formation of the Anyue giant gas field. *Russian Geology and Geophysics*, **61**, 478–494, https://doi.org/10.15372/rgg2020122

Kahoui, M., Mahdjoub, Y. and Kaminsky, F.V. 2008. Possible primary sources of diamond in the North African diamondiferous province. *Geological Society, London,*

Special Publications, **297**, 77–109, https://doi.org/10.1144/SP297.5

Kaye, G.W.C. and Laby, T.H. 1986. *Tables of Physical and Chemical Constants and Some Mathematical Functions*, 15th edn. Longman & Co., New York.

Klein, F., Bach, W. and McCollom, T.M. 2013. Compositional controls on hydrogen generation during serpentinization of ultramafic rocks. *Lithos*, **178**, 55–69, https://doi.org/10.1016/j.lithos.2013.03.008

Klein, F., Tarnas, J.D. and Bach, W. 2020. Abiotic sources of molecular hydrogen on Earth. *Elements*, **16**, 19–24, https://doi.org/10.2138/gselements.16.1.19

Labou, I., Benoit, M. *et al*. 2020. Petrological and geochemical study of Birimian ultramafic rocks within the West African Craton: insights from Mako (Senegal) and Loraboué (Burkina Faso) lherzolite/harzburgite/wehrlite associations. *Journal of African Earth Sciences*, **162**, https://doi.org/10.1016/j.jafrearsci.2019.103677

Lazar, C. 2020. Using silica activity to model redox-dependent fluid compositions in serpentinites from 100 to 700°C and from 1 to 20 kbar. *Journal of Petrology*, **61**, https://doi.org/10.1093/petrology/egaa101

Lesquer, A. and Moussine-Pouchkine, A. 1980. Les anomalies gravimetriques de la boucle du Niger. Leur signification dans le cadre de l'orogenese panafricaine. *Canadian Journal of Earth Sciences*, **17**, 1538–1545, https://doi.org/10.1139/e80-161

Libby, J., Groves, D.I. and Vearncombe, J.R. 1991. The nature and tectonic significance of the crustal-scale Koolyanobbing shear zone, Yilgarn Craton, Western Australia. *Australian Journal of Earth Sciences*, **38**, 229–245, https://doi.org/10.1080/08120099108727967

Lodhia, B.H. and Clark, S.R. 2022. Computation of vertical fluid mobility of CO_2, methane, hydrogen and hydrocarbons through sandstones and carbonates. *Scientific Reports*, **12**, https://doi.org/10.1038/s41598-022-14234-6

Lopez-Lazaro, C., Bachaud, P., Moretti, I. and Ferrando, N. 2019. Predicting the phase behavior of hydrogen in NaCl brines by molecular simulation for geological applications. *Bulletin de la Société géologique de France*, **190**, 1–15, https://doi.org/10.1051/bsgf/2019008

Magoon, L.B. and Dow, W.G. 1994. The petroleum system. *AAPG Memoir,* **60**, 3–24.

Maiga, O., Deville, E., Laval, J., Prinzhofer, A. and Diallo, A.B. 2023. Characterization of the spontaneously recharging natural hydrogen reservoirs of Bourakebougou in Mali. *Scientific Reports*, **13**, 11876, https://doi.org/10.1038/s41598-023-38977-y

Manuella, F.C. and Carbone, S. 2019. The identity of petrophysical properties of oceanic serpentinites and continental granitoids: implications for the recognition of buried hydrocarbon-bearing serpentinite geobodies. *Geotectonics*, **53**, 239–250, https://doi.org/10.1134/S0016852119020055

Monge, A.M. and Vayssaire, A. 2022. A review of some aspects of the molecular hydrogen transport behavior in the subsurface. Presented at the EAGE Annual 83rd Conference and Exhibition, Madrid, Spain, https://doi.org/10.3997/2214-4609.202210914

Montel, F., Caillet, G., Pucheu, A. and Caltagirone, J.P. 1993. Diffusion model for predicting reservoir gas losses. *Marine and Petroleum Geology*, **10**, 51–57, https://doi.org/10.1016/0264-8172(93)90099-E

Natural Hydrogen Energy LLC. 2019. Read more about natural hydrogen and our project [Home Page], http://nh2e.com/ [last accessed 15 February 2023]

Naylor, M. and Sinclair, H.D. 2008. Pro- vs. retro-foreland basins. *Basin Research*, **20**, 285–303, https://doi.org/10.1111/j.1365-2117.2008.00366.x

Nelson, P.H. 2009. It's A Small World After All – The Pore Throat Size Spectrum. *Search and Discovery*, **#50218**, https://www.searchanddiscovery.com/pdfz/documents/2009/50218nelson/ndx_nelson.pdf.html.

Nelson, J.S. and Simmons, E.C. 1995. Diffusion of methane and ethane through the reservoir cap rock: implications for the timing and duration of catagenesis. *AAPG Bulletin*, **79**, 1064–1073, https://doi.org/10.1306/8d2b21cd-171e-11d7-8645000102c1865d

Peng, P., Mitchell, R.N. and Chen, Y. 2022. Earth's one-of-a-kind fault: the Tanlu fault. *Terra Nova*, **34**, 381–394, https://doi.org/10.1111/ter.12611

Perera, M.S.A. 2023. A review of underground hydrogen storage in depleted gas reservoirs: insights into various rock-fluid interaction mechanisms and their impact on the process integrity. *Fuel*, **334**, https://doi.org/10.1016/j.fuel.2022.126677

Prinzhofer, A., Tahara Cissé, C.S. and Diallo, A.B. 2018. Discovery of a large accumulation of natural hydrogen in Bourakebougou (Mali). *International Journal of Hydrogen Energy*, **43**, 19315–19326, https://doi.org/10.1016/j.ijhydene.2018.08.193

Ranganai, R.T. 2012. Gravity and aeromagnetic studies of the Filabusi Greenstone Belt, Zimbabwe Craton: regional and geotectonic implications. *International Journal of Geosciences*, **3**, 1048–1064, https://doi.org/10.4236/ijg.2012.35106

Rezaei, A., Hassanpouryouzband, A., Molnar, I., Derikvand, Z., Haszeldine, R.S. and Edlmann, K. 2022. Relative permeability of hydrogen and aqueous brines in sandstones and carbonates at reservoir conditions. *Geophysical Research Letters*, **49**, https://doi.org/10.1029/2022GL099433

Rintamäki, A. 2016. *Serpentinization and carbonation of the komatiitic rocks in the Komati Complex, Barberton greenstone belt, South Africa*. MSc thesis, University of Helsinki.

Rostirolla, S.P., Mancini, F., Rigoti, A. and Kraft, R.P. 2003. Structural styles of the intracratonic reactivation of the Perimbó fault zone, Paraná basin, Brazil. *Journal of South American Earth Sciences*, **16**, 287–300, https://doi.org/10.1016/S0895-9811(03)00065-8

Rouméjon, S., Cannat, M., Agrinier, P., Godard, M. and Andreani, M. 2015. Serpentinization and fluid pathways in tectonically exhumed peridotites from the Southwest Indian Ridge (62–65°E). *Journal of Petrology*, **56**, 703–734, https://doi.org/10.1093/petrology/egv014

Roy, S., Raju, R., Chuang, H.F., Cruden, B.A. and Meyyappan, M. 2003. Modeling gas flow through microchannels and nanopores. *Journal of Applied Physics*, **93**, 4870–4879, https://doi.org/10.1063/1.1559936

Rüpke, L.H. and Hasenclever, J. 2017. Global rates of mantle serpentinization and H_2 production at oceanic transform faults in 3-D geodynamic models. *Geophysical*

Research Letters, **44**, 6726–6734, https://doi.org/10.1002/2017GL072893

Sakhaee-Pour, A. and Alessa, S. 2022. Hydrogen permeability in subsurface. *International Journal of Hydrogen Energy*, **47**, 27071–27079, https://doi.org/10.1016/j.ijhydene.2022.06.042

Sauvage, J.-F. and Sauvage, M. 1992. Tectonique, neotectonique et phenomenes ignes a l'extremite est du fosse de Nara (Mali): Daounas et lac Faguibine. *Journal of African Earth Sciences*, **15**, 11–33, https://doi.org/10.1016/0899-5362(92)90003-U

Sheldon, H.A., Barnicoat, A.C. and Ord, A. 2006. Numerical modelling of faulting and fluid flow in porous rocks: an approach based on critical state soil mechanics. *Journal of Structural Geology*, **28**, 1468–1482, https://doi.org/10.1016/j.jsg.2006.03.039

Sleep, N.H., Meibom, A., Fridriksson, T., Coleman, R.G. and Bird, D.K. 2004. H_2-rich fluids from serpentinization: geochemical and biotic implications. *Proceedings of the National Academy of Science*, **101**, 12818–12823, https://doi.org/10.1073/pnas.0405289101

Stalker, L., Talukder, A., Strand, J., Josh, M. and Faiz, M. 2022. Gold (hydrogen) rush: risks and uncertainties in exploring for naturally occurring hydrogen. *The APPEA Journal*, **62**, 361–380, https://doi.org/10.1071/AJ21130

Svensen, H., Dysthe, D.K., Bandlien, E.H., Sacko, S., Coulibaly, H. and Planke, S. 2003. Subsurface combustion in Mali: refutation of the active volcanism hypothesis in West Africa. *Geology*, **31**, 581–584, https://doi.org/10.1130/0091-7613(2003)031<0581:SCIMRO>2.0.CO;2

Toft, P.B., Arkani-Hamed, J. and Haggerty, S.E. 1990. The effects of serpentinization on density and magnetic susceptibility: a petrophysical model. *Physics of the Earth and Planetary Interiors*, **65**, 137–157, https://doi.org/10.1016/0031-9201(90)90082-9

Traore, A.Z., Bokar, H., Sidibe, A., Upton, K., Ó Dochartaigh, B.É. and Bellwood-Howard, I. 2018. Hydrogeology of Mali, https://earthwise.bgs.ac.uk/index.php/Hydrogeology_of_Mali [last accessed 09 January 2024]

Ulrich, M., Muñoz, M., Boulvais, P., Cathelineau, M., Cluzel, D., Guillot, S. and Picard, C. 2020. Serpentinization of New Caledonia peridotites: from depth to (sub-)surface. *Contributions to Mineralogy and Petrology*, **175**, https://doi.org/10.1007/s00410-020-01713-0

US DoE. 2020. The Department of Energy Hydrogen Program Plan, United States Department of Energy, https://www.hydrogen.energy.gov/pdfs/hydrogen-program-plan-2020.pdf

Vearncombe, J.R., Barton, J.M., Jr, van Reenen, D.D., Phillips, G.N. and Wilson, A.H. 1986. Greenstone Belts: Their Components and Structure. Presented at the Workshop on the Tectonic Evolution of Greenstone Belts, 16–18 January 1986, Houston, Texas, 19–25.

Vitale Brovarone, A., Sverjensky, D.A., Piccoli, F., Ressico, F., Giovannelli, D. and Daniel, I. 2020. Subduction hides high-pressure sources of energy that may feed the deep subsurface biosphere. *Nature Communications*, **11**, https://doi.org/10.1038/s41467-020-17342-x

Worman, S.L., Pratson, L.F., Karson, J.A. and Klein, E.M. 2016. Global rate and distribution of H_2 gas produced by serpentinization within oceanic lithosphere. *Geophysical Research Letters*, **43**, 6435–6443, https://doi.org/10.1002/2016GL069066

Zgonnik, V. 2020. The occurrence and geoscience of natural hydrogen: a comprehensive review. *Earth-Science Reviews*, **203**, https://doi.org/10.1016/j.earscirev.2020.103140

Zhao, C., Hobbs, B.E., Mühlhaus, H.B., Ord, A. and Lin, G. 2003. Convective instability of 3-D fluid-saturated geological fault zones heated from below. *Geophysical Journal International*, **155**, 213–220, https://doi.org/10.1046/j.1365-246X.2003.02032.x

Zongo, W.P.P., Wenmenga, U. and Koffi, Y.H. 2016. Mineralogical and petrochemical characterization of Tambogo serpentinites: Birimian greenstone belt of Kaya-Goren, Burkina Faso. *Bulletin de l'Institut Scientifique, Rabat, Section Sciences de la Terre*, **38**, 81–94.